Simulations of Coulomb systems with slab geometry using an efficient 3D Ewald summation method

Alexandre P. dos Santos, Matheus Girotto, and Yan Levin

Articles you may be interested in

Communication: Constant uncertainty molecular dynamics: A simple and efficient algorithm to incorporate quantum nature into a real-time molecular dynamics simulation
The Journal of Chemical Physics **145**, 171101171101 (2016); 10.1063/1.4966917

A new discretization for the polarizable continuum model within the domain decomposition paradigm
The Journal of Chemical Physics **144**, 054101054101 (2016); 10.1063/1.4940136

An automated nudged elastic band method
The Journal of Chemical Physics **145**, 094107094107 (2016); 10.1063/1.4961868

Energy landscapes and persistent minima
The Journal of Chemical Physics **144**, 054109054109 (2016); 10.1063/1.4941052

Communication: Inverse design for self-assembly via on-the-fly optimization
The Journal of Chemical Physics **145**, 111101111101 (2016); 10.1063/1.4962754

On metastability and Markov state models for non-stationary molecular dynamics
The Journal of Chemical Physics **145**, 174103174103 (2016); 10.1063/1.4966157

Simulations of Coulomb systems with slab geometry using an efficient 3D Ewald summation method

Alexandre P. dos Santos,[a)] Matheus Girotto,[b)] and Yan Levin[c)]
*Instituto de Física, Universidade Federal do Rio Grande do Sul, Caixa Postal 15051, CEP 91501-970,
Porto Alegre, RS, Brazil*

We present a new approach to efficiently simulate electrolytes confined between infinite charged walls using a 3d Ewald summation method. The optimal performance is achieved by separating the electrostatic potential produced by the charged walls from the electrostatic potential of electrolyte. The electric field produced by the 3d periodic images of the walls is constant inside the simulation cell, with the field produced by the transverse images of the charged plates canceling out. The *non-neutral* confined electrolyte in an external potential can be simulated using 3d Ewald summation with a suitable renormalization of the electrostatic energy, to remove a divergence, and a correction that accounts for the conditional convergence of the resulting lattice sum. The new algorithm is at least an order of magnitude more rapid than the usual simulation methods for the slab geometry and can be further sped up by adopting a particle–particle particle–mesh approach. © *2016 AIP Publishing LLC.* [http://dx.doi.org/10.1063/1.4945560]

INTRODUCTION

Study of electrolyte solutions is of paramount importance in physics, chemistry, and biology. Electrolytes are fundamental to human physiology,[1] but also play an important role in systems as distinct as water soluble paints,[2] cement,[3] supercapacitors,[4,5] etc. The long range nature of the Coulomb force makes it very difficult to obtain a quantitative understanding of these systems. The well known Poisson-Boltzmann (PB) equation can provide valuable insights for weakly interacting Coulomb systems for which electrostatic correlations are negligible.[6] However, many interesting phenomena, such as like-charge attraction[7–11] and charge reversal,[12–15] appear when PB equation loses its validity. To study such systems a number of theoretical approaches have been introduced. These fall into three main categories: integral equations,[12,16,17] field theory,[18,19] and density functional theory.[8,20] All of these methods, however, rely on approximations which must be tested "experimentally." The only "exact" quantitative approach for studying 3d Coulomb systems relies on Molecular Dynamics (MD) or Monte Carlo (MC) simulations.[21] Unfortunately, because of the long range interaction, simulations of Coulomb systems are notoriously challenging. The difficulty arises because unlike for systems with short range forces, one cannot use periodic boundary conditions for the simulation box. Instead, an infinity of periodic replicas of the simulation cell must be constructed. Each ion in the principal simulation cell interacts with an infinite number of images of all the other ions. In order to efficiently sum over the replicas, Ewald summation methods have been developed.[22–24] These methods rely on splitting the interaction potential into short and long range contributions, so that the short range part can be rapidly calculated in the real space, while the long range part can be efficiently summed in the reciprocal, Fourier space. Ewald summation methods are particularly useful for 3d isotropic systems. However, when a system has a reduced 2d symmetry, application of Ewald summation techniques becomes more challenging. The difficulty in these cases is the appearance of Bessel function in 2d Fourier transforms, contrary to a simple exponential present in 3d, leading to a very slow convergence.[25,26] This problem not withstanding, there is a great practical importance to understand systems with reduced symmetry. These relate to the class of problems with characteristic slab geometry—water and ionic liquids confined in thin films,[27–29] charged nanopores,[30–32] self-assembled monolayers,[33] polymer layers,[34] heterogeneous charged surfaces,[35–37] just to cite a few examples.

The efficiency of Ewald-like 2d and 1d methods is not nearly as high as for isotropic 3d systems. The slow convergence rate was a subject of extensive studies.[38,39] A number of different approaches have been tried to overcome this difficulty.[40–45] In the present paper we will introduce a new method to simulate electrolyte solutions confined by the charged walls. To avoid the slow convergence of 2d Ewald approach, we will use 3d Ewald summation. This means that the system will be replicated in all three dimensions. In reality, however, we are only interested in 2d (x, y) part of the replication, with the transverse z-replicas being an artifact of the 3d Ewald summation. To diminish the effect of z-replicas, we will include a vacuum region on both sides of the slab within the simulation cell. This, however, is not sufficient to adopt 3d Ewald summation to 2d geometry. The conditional convergence of the lattice sum still results in a surface contribution to the total electrostatic energy which depends on the aspect ratio of the macroscopic system (sum

---
a)alexandre.pereira@ufrgs.br
b)matheus.girotto@ufrgs.br
c)levin@if.ufrgs.br

of all the replicas). Since we are interested in an infinite slab, the aspect ratio should be such that the x and y sides of the slab are infinitely bigger than the slab width (z-direction). For a conditionally convergent lattice sum this means that the summation has to be first done over x and y directions, and then over z-direction. This important point was discussed by Smith[46] and implemented in simulations by Yeh and Berkowitz[42] (YB). The approach of YB is quite simple. If the system consists of electrolyte and charged plates, one can discretize the surface charge and apply 3d Ewald summation method, with an additional surface correction, to the whole system, i.e., electrolyte and the wall charges. Clearly this is not very efficient since it requires to include in the lattice sum the surface charges which are fixed throughout the simulation. Since the electric field produced by the plates is constant, it should be possible to separate it from the rest of the system, allowing the ions to move in a fixed external potential produced by the plates, which has a simple linear form. The difficulty with this approach is that a system of only ions, without the wall charges, is not charge neutral, so that the lattice sum will diverge. In this paper we will show, however, that this divergence can be renormalized away, allowing us to construct a very fast and efficient algorithm for simulating ionic systems in a slab geometry.

METHOD

The idea of the present method is to consider the electrostatic potential produced by the plates as an external scalar field acting on all the ions inside the simulation cell. As we intend to use the 3d Ewald summation to accelerate the simulations, we must consider the replicas of the plates in z-direction in addition to the replicas in x and y-directions. The electric fields of two infinite uniformly charged plates are $2\pi\sigma_1/\epsilon_w$ and $2\pi\sigma_2/\epsilon_w$, where σ_1 is the charge density of the left plate and σ_2 of the right plate, and ϵ_w is the dielectric constant of the medium, normally water. Both fields are orthogonal to the plates. The replication of the simulation cell in the x and y directions will naturally result in 2 infinite plates. However, the replication of the simulation cell in the z direction will produce an infinite array of such infinite surfaces, see Fig. 1. We note, however, that the electric fields that these z-images of the plates produce on the ions inside the

simulation box cancel out, so that the ions in the cell feel only the electric fields of the bounding walls and of their x and y replicas. These are precisely the electric fields of the infinite charged plates: $2\pi\sigma_1/\epsilon_w$ and $2\pi\sigma_2/\epsilon_w$. We can, therefore, separate the electric field (or equivalently the electrostatic potential) produced by the charged walls and their images from the field produced by the ions and their images. For more complicated geometries, such as a cylindrical charged nanopore, additional care is required to account for the electric field produced by the periodic replicas of the charged cylinder. The difficulty now is that the replicated system of just ions is no longer charge neutral, so that the electrostatic potential produced by the images of all the ions will diverge. We will show, however, that this divergence can be renormalized away, allowing us to study a non-neutral periodic charged system.

Consider a system of particles of charges q^j located at random positions r^j inside a box of sides L_x, L_y and L_z. The system in general is not charge neutral. Let us consider, without loss of generality, $L_x = L_y = L$. The system is now replicated infinitely in all directions. The replication vector is defined as $r_{ep} = (Ln_1, Ln_2, L_z n_3)$, where $n's$ are integers. In Fig. 2 we show the replicated system. The electrostatic potential generated by the ions and all the images at a point P, located at some random position r in the simulation box, can be written as

$$\phi(r) = \sum_n^\infty \sum_{j=1}^N \int \frac{\rho^j(s)}{\epsilon_w|r - s|} d^3 s, \qquad (1)$$

where $\rho^j(s) = q^j \delta(s - r^j - r_{ep})$ is the charge density of q^j and its replicas. The vector $n = (n_1, n_2, n_3)$ represents all the replicas, and the simulation box corresponds to $(0,0,0)$. The 3d Ewald summation[21] is a very efficient method for performing summation over all the replicas. The idea is to place a neutralizing Gaussianly distributed charge on top of each ion and then subtract the potential produced by the Gaussian charges from the total potential. The fundamental observation is that if the charge of each ion is neutralized by the Gaussian charge, the resulting potential will be short ranged and can be easily accounted for using simple periodic boundary conditions. On the other hand, the potential of the Gaussian charges can be efficiently calculated using the Fourier representation of the charge density. In fact the
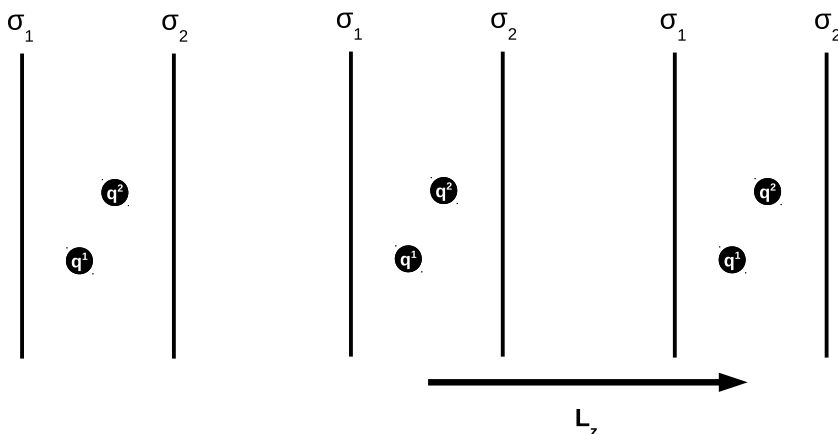

FIG. 1. 3d replicated system. Note that inside the central simulation cell the electric field produced by the z-replication of charged walls cancels out.
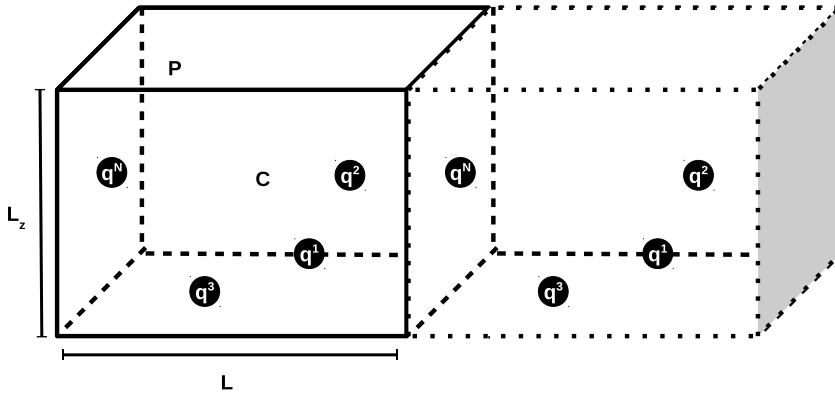
FIG. 2. The simulation box with randomly positioned charges and one of its replicas. The point C represents the center of the simulation box, where the origin is located, and P is an arbitrary point.

distribution does not need to be Gaussian, but this is the most common choice.[47]

The electrostatic potential after adding and subtracting the Gaussian charges is

$$\phi(\boldsymbol{r}) = \sum_{\boldsymbol{n}}^{\infty} \sum_{j=1}^{N} \int \frac{\rho^j(\boldsymbol{s}) - \rho_G^j(\boldsymbol{s})}{\epsilon_w |\boldsymbol{r} - \boldsymbol{s}|} d^3\boldsymbol{s} + \sum_{\boldsymbol{n}}^{\infty} \sum_{j=1}^{N} \int \frac{\rho_G^j(\boldsymbol{s})}{\epsilon_w |\boldsymbol{r} - \boldsymbol{s}|} d^3\boldsymbol{s},$$
(2)

where $\rho_G^j(\boldsymbol{s}) = q^j(\kappa_e^3/\sqrt{\pi^3}) \exp(-\kappa_e^2|\boldsymbol{s} - \boldsymbol{r}^j - \boldsymbol{r}_{ep}|^2)$ and κ_e is a dumping parameter. The potential can be written as

$$\phi(\boldsymbol{r}) = \sum_{\boldsymbol{n}}^{\infty} \sum_{j=1}^{N} q^j \frac{\text{erf}(\kappa_e|\boldsymbol{r} - \boldsymbol{r}^j - \boldsymbol{r}_{ep}|)}{\epsilon_w |\boldsymbol{r} - \boldsymbol{r}^j - \boldsymbol{r}_{ep}|}$$

$$+ \sum_{\boldsymbol{n}}^{\infty} \sum_{j=1}^{N} q^j \frac{\text{erfc}(\kappa_e|\boldsymbol{r} - \boldsymbol{r}^j - \boldsymbol{r}_{ep}|)}{\epsilon_w |\boldsymbol{r} - \boldsymbol{r}^j - \boldsymbol{r}_{ep}|}.$$
(3)

Using the Fourier transform the expression above can be written as

$$\phi(\boldsymbol{r}) = \sum_{\boldsymbol{k}=0}^{\infty} \sum_{j=1}^{N} \frac{4\pi q^j}{\epsilon_w V |\boldsymbol{k}|^2} \exp[-\frac{|\boldsymbol{k}|^2}{4\kappa_e^2} + i\boldsymbol{k} \cdot (\boldsymbol{r} - \boldsymbol{r}^j)]$$

$$+ \sum_{j=1}^{N} q^j \frac{\text{erfc}(\kappa_e|\boldsymbol{r} - \boldsymbol{r}^j|)}{\epsilon_w |\boldsymbol{r} - \boldsymbol{r}^j|},$$
(4)

where $\boldsymbol{k} = (\frac{2\pi}{L}n_1, \frac{2\pi}{L}n_2, \frac{2\pi}{L_z}n_3)$. In the second term of Eq. (2) we have removed the summation over replicas, considering only the main simulation box, $\boldsymbol{n} = (0,0,0)$, with the usual periodic boundary condition. This is justified if κ_e is chosen to be sufficiently large, so that $\text{erfc}(\kappa_e|\boldsymbol{r}|)$ decays rapidly, and the minimum image convention (periodic boundary condition) can be used. In practice we set $\kappa_e = 5/L$, if $L < L_z$ or $\kappa_e = 5/L_z$, if $L > L_z$.

For $\boldsymbol{k} = (0,0,0)$ the first term of Eq. (4) is singular. This term has been a topic of extensive discussions.[21,48–50] In order to treat it, some authors argue that we must consider the induced surface charge at the boundary of an infinite system. They argue that this boundary term can be neglected if the exterior medium is a metal, so called, tinfoil boundary condition. However, for an infinite system, there is no boundary. Furthermore, introduction of a boundary is inconsistent with the periodicity of the system used to perform the Ewald summation. Clearly the lattice sum can be performed in real space, and although it is conditionally convergent, for a specific method of

summation—spherical or planewise—the result will be well defined and should agree with the Ewald summation method. If the $\boldsymbol{k} = (0,0,0)$ term is neglected, the real space and Ewald method calculations will disagree. Fortunately, for isotropic systems neglecting the $\boldsymbol{k} = (0,0,0)$ term appears to introduce only small errors. However, for systems with a slab geometry neglect of $\boldsymbol{k} = (0,0,0)$ term can lead to very significant errors. These observations are consistent with the results of Nymand and Linse (NL),[51] who compared the electrostatic potentials for an isotropic neutral system using direct real space summation and the Ewald method, see Table 1 of Ref. 51. For homogeneous bulk systems (which correspond to spherical summation of replicas) they observed that the energy contribution of the singular term is small *on average*. However, NL did not consider slab geometry—which corresponds to planewise summation of replicas—in which case neglect of the singular terms can result in very large errors.[42] Let us now consider the singular term in more detail. Neglecting the prefactors, the $\boldsymbol{k} = (0,0,0)$ term can be written as

$$\lim_{\boldsymbol{k} \to 0} \sum_{j=1}^{N} \frac{q^j}{|\boldsymbol{k}|^2} \exp[-\frac{|\boldsymbol{k}|^2}{4\kappa_e^2}] \exp[+i\boldsymbol{k} \cdot (\boldsymbol{r} - \boldsymbol{r}^j)].$$
(5)

Now, let us expand the exponentials and keep only the singular terms,

$$\lim_{\boldsymbol{k} \to 0} \sum_{j=1}^{N} q^j \frac{1}{|\boldsymbol{k}|^2} - \sum_{j=1}^{N} q^j \frac{1}{4\kappa_e^2} + \lim_{\boldsymbol{k} \to 0} \sum_{j=1}^{N} q^j \frac{i\boldsymbol{k} \cdot (\boldsymbol{r} - \boldsymbol{r}^j)}{|\boldsymbol{k}|^2}$$

$$- \lim_{\boldsymbol{k} \to 0} \sum_{j=1}^{N} q^j \frac{[\boldsymbol{k} \cdot (\boldsymbol{r} - \boldsymbol{r}^j)]^2}{2|\boldsymbol{k}|^2}.$$
(6)

In a charge neutral system, $\sum_j q^j = 0$, the first two terms are zero. For a non-neutral system, however, they are infinite. On the other hand, they are independent of $\boldsymbol{r}$, and can be renormalized away by simply redefining the zero of the potential. The third and fourth terms of expression (6) are position dependent and require greater care when calculating the limit $\boldsymbol{k} \to 0$. We first observe that the singular behavior of the $\boldsymbol{k} \to 0$ is a consequence of the large distance behavior of the lattice sum. To properly account for this limit we rewrite the third and the fourth terms of expression (6) using Dirac delta function. The third term can then be

expressed as

$$S_3 = \sum_{j=1}^{N} q^j \int_{-\infty}^{+\infty} \delta(\mathbf{k}) \frac{i\mathbf{k} \cdot (\mathbf{r} - \mathbf{r}^j)}{|\mathbf{k}|^2} d^3k, \qquad (7)$$

with the following representation of $\delta(\mathbf{k}) = \frac{1}{(2\pi)^3} \int_{-H}^{H} e^{i\mathbf{k}\cdot\mathbf{p}} d^3p$.

The limits of integration, $-\mathbf{H}$ and $\mathbf{H}$, where $\mathbf{H} = (H_1, H_2, H_3)$ correspond to the way that the sums are performed in the real space. For example, if we replicate the simulation cell in a spherically symmetric fashion, then $H_1 = lim_{m\to\infty} mL_x$, $H_2 = lim_{m\to\infty} mL_y$, and $H_3 = lim_{m\to\infty} mL_y$, that is all sides diverge at the same rate. On the other hand for a slab geometry H_1 and H_2 limits should go to infinity much faster than H_3. In general it is convenient to define $H_1 = \alpha_1 L_c$, $H_2 = \alpha_2 L_c$, and $H_3 = \alpha_3 L_c$, where L_c is some characteristic macroscopic length scale. The ratio of $\alpha's$ then corresponds to the aspect ratio of the macroscopic system, i.e., the simulation cell and all of its replicas. The integral over p_1, p_2, and p_3 can be performed explicitly yielding the following representation of the delta function:

$$\delta(\mathbf{k}) = \frac{1}{(2\pi)^3} \prod_{i=1}^{3} \int_{-\alpha_i \frac{L_c}{2}}^{\alpha_i \frac{L_c}{2}} e^{ik_i p_i} dp_i = \frac{1}{\pi^3} \prod_{i=1}^{3} \frac{\sin(k_i \alpha_i L_c/2)}{k_i}. \qquad (8)$$

This representation encodes the large distance behavior of the lattice sum and is at the heart of the singular behavior of $\mathbf{k} \to 0$ limit. Eq. (7) can then be written as $S_3 = \sum_{j=1}^{N} q_j \mathbf{D} \cdot (\mathbf{r} - \mathbf{r}^j)$, where the components of the vector $\mathbf{D}$ are

$$D_n = \frac{i}{\pi^3} \int_{-\infty}^{+\infty} \frac{k_n}{|\mathbf{k}|^2} \prod_{j=1}^{3} \frac{\sin(k_j \alpha_j L_c/2)}{k_j} d^3k, \qquad (9)$$

which by symmetry integrate to zero, $D_n = 0$, so that $S_3 = 0$.

The fourth singular term of expression (6) is

$$S_4 = -\sum_{j=1}^{N} q^j \int_{-\infty}^{+\infty} \delta(\mathbf{k}) \frac{[\mathbf{k} \cdot (\mathbf{r} - \mathbf{r}^j)]^2}{2|\mathbf{k}|^2} d^3k. \qquad (10)$$

Again using the representation of the delta function it can be rewritten as

$$S_4 = -\sum_{j=1}^{N} \frac{q^j}{2\pi^3} \sum_{n=1}^{3} B_n (r_n - r_n^j)^2, \qquad (11)$$

where the index n corresponds to the x, y, and z components of the vector $\mathbf{r}$ and

$$B_n = \int_{-\infty}^{+\infty} d^3k \frac{k_n^2}{|\mathbf{k}|^2} \prod_{j=1}^{3} \frac{\sin(k_j \alpha_j L_c/2)}{k_j}. \qquad (12)$$

Using the identity

$$\frac{1}{|\mathbf{k}|^2} = \int_0^\infty dt \, e^{-tk^2}, \qquad (13)$$

the coefficients B_n can be simplified to[46]

$$B_1 = \frac{\pi^{\frac{5}{2}}}{2} \int_0^{+\infty} \frac{\alpha_{13} e^{-\frac{\alpha_{13}^2}{4t}} \text{erf}(\frac{\alpha_{23}}{2\sqrt{t}}) \text{erf}(\frac{1}{2\sqrt{t}})}{t^{\frac{3}{2}}} dt, \qquad (14)$$

$$B_2 = \frac{\pi^{\frac{5}{2}}}{2} \int_0^{+\infty} \frac{\alpha_{23} e^{-\frac{\alpha_{23}^2}{4t}} \text{erf}(\frac{\alpha_{13}}{2\sqrt{t}}) \text{erf}(\frac{1}{2\sqrt{t}})}{t^{\frac{3}{2}}} dt, \qquad (15)$$

$$B_3 = \frac{\pi^{\frac{5}{2}}}{2} \int_0^{+\infty} \frac{e^{-\frac{1}{4t}} \text{erf}(\frac{\alpha_{13}}{2\sqrt{t}}) \text{erf}(\frac{\alpha_{23}}{2\sqrt{t}})}{t^{\frac{3}{2}}} dt, \qquad (16)$$

where $\alpha_{ij} = \alpha_i/\alpha_j$ are the aspect ratios of the macroscopic system. The coefficients B_n can now be easily calculated using numerical integration. For a spherically symmetric summation of replicas, the aspect ratios are $\alpha_{13} = L_x/L_z$ and $\alpha_{23} = L_y/L_z$. On the other hand, for a planewise summation of a slab geometry, $\alpha_{13} \to \infty$ and $\alpha_{23} \to \infty$. In this case the integrals can be performed explicitly[46] yielding $B_1 = B_2 = 0$, and $B_3 = \pi^3$.

Separating the $\mathbf{k} = \mathbf{0}$ term from the $\mathbf{k}$-vector summation, Eq. (4) can now be rewritten as

$$\Delta\phi(\mathbf{r}) = \sum_{\mathbf{k}\neq\mathbf{0}}^{\infty} \sum_{j=1}^{N} \frac{4\pi q^j}{\epsilon_w V |\mathbf{k}|^2} \exp[-\frac{|\mathbf{k}|^2}{4\kappa_e^2} + i\mathbf{k} \cdot (\mathbf{r} - \mathbf{r}^j)]$$
$$- \sum_{j=1}^{N} \sum_{n=1}^{3} \frac{2q^j}{\epsilon_w V \pi^2} B_n (r_n - r_n^j)^2$$
$$+ \sum_{j=1}^{N} q^j \frac{\text{erfc}(\kappa_e |\mathbf{r} - \mathbf{r}^j|)}{\epsilon_w |\mathbf{r} - \mathbf{r}^j|}, \qquad (17)$$

where Δ corresponds to the renormalization of the potential in Eq. (4)—subtraction of infinite constants. As a test of the modified Ewald summation formula for a non-neutral system, Eq. (17), we calculate the electrostatic potential difference between a random position $\mathbf{r}$ and the center of the simulation box, $\mathbf{0}$. Note that although the electrostatic potential is divergent for a non-neutral periodic system, the potential difference is well defined. We calculate the renormalized electrostatic potential produced by the two charges $q_1 = q_2 = |e|$, where e is the electron charge, located at random positions. We set $L_x = L_y = L = 1$ Å and $L_z = 2$ Å. The spherical replication of the rectangular simulation box will result in an infinite system with an aspect ratio of $\alpha_{13} = 1/2$ and $\alpha_{23} = 1/2$, leading to parameters $B_1 = B_2 = 13.5158$ and $B_3 = 3.9746$. Using Eq. (17), we find the converged value $\Delta\phi = \phi(\mathbf{r}) - \phi(\mathbf{0})$, to 2-decimal place accuracy, using ≈ 250 k-vectors spherically summed. In real space, using the explicit summation, Eq. (1), we find exactly the same converged value for $\Delta\phi(\mathbf{r})$, the convergence, however, is much slower, so that to get a 2-decimal place accuracy requires summation of over $\approx 19\,700$ n-vectors. For isotropic bulk simulations, the energy contribution due to the singular term appears to be small *on average*. This can account for the prevalent use of "tinfoil" boundary conditions which are claimed to eliminate the $\mathbf{k} = \mathbf{0}$ term. However, in order to properly describe an electrostatic system in thermodynamic limit—in particular an inhomogeneous one—using simulations based on the periodic cell replication, the singular term is important and cannot, in general, be neglected.

In the slab geometry we want to calculate the potential difference when the simulation box is replicated in the x and y directions only. Again we will use the modified 3d Ewald summation given by Eq. (17). This means that the box will be

replicated in all 3 dimensions. However, the replication in the x and y directions should be performed at a rate much faster than in the z direction. This leads to $B_1 = B_2 = 0$, and $B_3 = \pi^3$ and Eq. (17) becomes

$$\Delta\phi(\boldsymbol{r}) = \sum_{\boldsymbol{k}\neq\boldsymbol{0}}^{\infty}\sum_{j=1}^{N}\frac{4\pi q^j}{\epsilon_w V|\boldsymbol{k}|^2}\exp[-\frac{|\boldsymbol{k}|^2}{4\kappa_e^2} + i\boldsymbol{k}\cdot(\boldsymbol{r}-\boldsymbol{r}^j)]$$
$$- \sum_{j=1}^{N}\frac{2\pi q^j}{\epsilon_w V}(r_3 - r_3^j)^2 + \sum_{j=1}^{N} q^j\frac{\text{erfc}(\kappa_e|\boldsymbol{r}-\boldsymbol{r}^j|)}{\epsilon_w|\boldsymbol{r}-\boldsymbol{r}^j|}. \tag{18}$$

Even though the contribution from the z-directional replicas is much smaller than from the x and y directional replicas, it is not negligible. In order to diminish the impact of z-replicas on the electrostatic potential, we must leave a sufficiently large vacuum region in the z-direction. To test Eq. (18) for a slab geometry, we study the same 2 particle system discussed earlier. Using Eq. (1) we can explicitly calculate the potential difference $\Delta\phi = \phi(\boldsymbol{r}) - \phi(\boldsymbol{0})$, when the simulation cell is replicated only in the x and y directions, $\boldsymbol{n} = (n_x, n_y, 0)$. The convergence is very slow requiring values of 2.5×10^6 replicas to get an accuracy of 2-decimal places.

To diminish the interaction with z-directional replicas, in order to use Eq. (18) for a slab geometry, we restrict positions of the charges and the vector $\boldsymbol{r}$ to the region $-\frac{L_z}{4} < z < \frac{L_z}{4}$ in the simulation cell, leaving the regions $-\frac{L_z}{2} < z < -\frac{L_z}{4}$ and $\frac{L_z}{4} < z < \frac{L_z}{2}$ empty. The calculated electrostatic potential difference is exactly the same as found using the real-space lattice summation. The same 2-decimal point accuracy, however, is achieved with only ≈ 630 k-vectors.

The renormalized electrostatic energy for a non-neutral slab system can now be calculated as $E = \frac{1}{2}\sum_{i=1}^{N} q^i\Delta\phi(\boldsymbol{r}^i)$,

$$E = \sum_{\boldsymbol{k}\neq\boldsymbol{0}}^{\infty}\frac{2\pi}{\epsilon_w V|\boldsymbol{k}|^2}\exp[-\frac{|\boldsymbol{k}|^2}{4\kappa_e^2}][A(\boldsymbol{k})^2 + B(\boldsymbol{k})^2]$$
$$+ \frac{2\pi}{\epsilon_w V}[M_z^2 - Q_t G_z] + \frac{1}{2}\sum_{i\neq j}^{N} q^i q^j\frac{\text{erfc}(\kappa_e|\boldsymbol{r}^i-\boldsymbol{r}^j|)}{\epsilon_w|\boldsymbol{r}^i-\boldsymbol{r}^j|}, \tag{19}$$

where

$$A(\boldsymbol{k}) = \sum_{i=1}^{N} q^i\cos(\boldsymbol{k}\cdot\boldsymbol{r}^i),$$

$$B(\boldsymbol{k}) = -\sum_{i=1}^{N} q^i\sin(\boldsymbol{k}\cdot\boldsymbol{r}^i),$$

$$M_z = \sum_{i=1}^{N} q^i r_3^i, \tag{20}$$

$$Q_t = \sum_{i=1}^{N} q^i,$$

$$G_z = \sum_{i=1}^{N} q^i(r_3^i)^2.$$

For a neutral system, $Q_t = 0$, and we recover the earlier expression for the electrostatic energy.[42]

We now apply the method developed above to a system of electrolyte confined between two charged walls. We set $L = 179$ Å and $L_z = 400$ Å. The ionic radius is 2 Å, while the separation between plates is 50 Å. The number of k-vectors is around 300. The equilibration is achieved with 1×10^6 MC steps, while the density profiles are obtained with 20 000 samples, each saved after 100 particle trial moves. As a first example, we set $\sigma_1 = 0.04$ C/m^2 and $\sigma_2 = -0.01$ C/m^2. For plate 1 we have 80 counterions of charge $-|e|$, while for plate 2, we have 20 counterions of charge $|e|$. In the MC Metropolis algorithm we use the energy expression Eq. (19), for the $N_c = 100$ ions, and the electrostatic energy of interaction between ions and the charged walls,

$$E_p = \frac{2\pi}{\epsilon_w}\sum_{i=1}^{N_c}(\sigma_2 - \sigma_1)r_3^i q^i. \tag{21}$$

To appreciate the power of the present method we compare it with the usual algorithm in which the surface charge is represented by 256 uniformly distributed point particles.[42] In this case we use Eq. (19) for a neutral system, considering all charged particles, including the ones on the plate surface, $Q_t = 0$. The result is shown in Fig. 3 and is indistinguishable from the non-neutral simulation method developed in the present paper. The gain in the simulation time is very substantial—a traditional simulation method took 20 times more CPU time than the algorithm developed in the present paper. Next we apply the new simulation method to the case of $\sigma_1 = \sigma_2$. This situation is particularly relevant for studying colloidal stability with the help of Derjaguin approximation.[52] We consider 500 mM of 2:1 or 4:1 dissociated electrolyte between charged walls. The electric fields produced by the plates cancel out. Therefore, the simulation is performed only with Eq. (19)—we do not need to take into account the plates in the calculations, except in order to obtain the number of plate counterions. For $\sigma_1 = \sigma_2 = -0.04$ C/m^2, we have 80 counterions of charge $2|e|$, for 2:1 case, and 40 counterions of charge $4|e|$, for 4:1 case. Using the same $L = 179$ Å and $L_z = 400$ Å, the ionic profiles and the integrated charges are
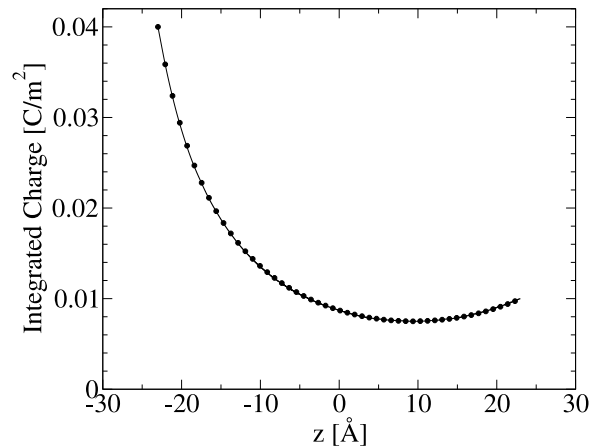

FIG. 3. Integrated charge between charged surfaces. Symbols represent the calculation using the modified (non-neutral) 3d Ewald approach, while line, the traditional method.[42] The difference is imperceptible.
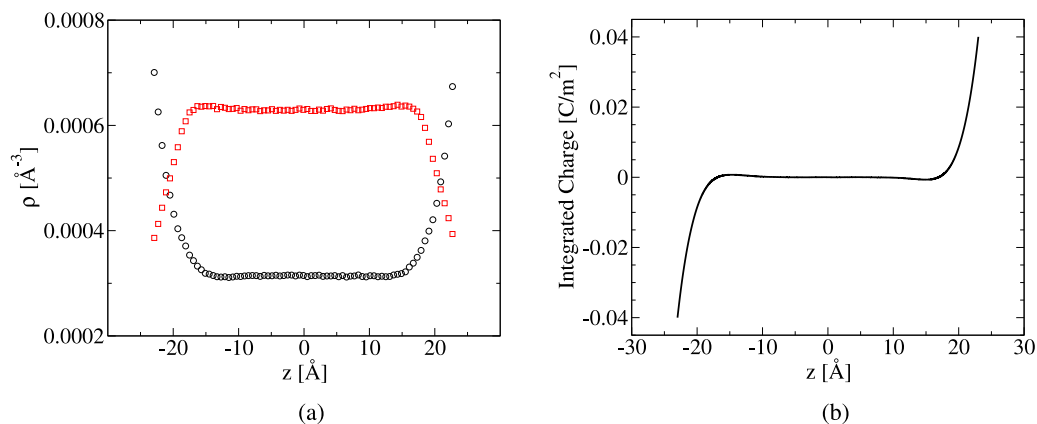
(a)

(b)

FIG. 4. (a) Density profiles of ions between equally charged surfaces confining 2:1 electrolyte—circles represent positive ions, while squares negative ones. (b) The integrated charge.

shown in Figs. 4 and 5. Observe that for 4:1 salt there is a significant charge inversion, so that the condensed counterions overcompensate the surface charge on the plates, see Fig. 5. This phenomenon can also occur with divalent counterions, but is much weaker, see Fig. 4. A study of such strongly

concentrated inhomogeneous charged systems is not very practical with other simulation methods.

CONCLUSIONS

We have developed a new approach for simulating electrolytes in a confined slab geometry. Our algorithm relies on 3d Ewald summation to properly account for the long range Coulomb interaction between the ions and the charged surfaces. The optimal performance of the method is achieved by separating the electrostatic potential produced by the charged walls from the potential produced by the electrolyte. The fundamental observation is that the electrostatic potential produced by the 3d periodic images of the plates has a simple linear form, with the electric field produced by the transverse images of the charged plates canceling out. This observation suggests that the ions and the charged surfaces can be treated separately. The difficulty, however, is that the system of only ions no longer respects the charge neutrality, with its electrostatic energy diverging. Nevertheless, we showed that a simple renormalization of the electrostatic potential cures the divergence, allowing us to consider a non-neutral system of ions moving in the field produced by the charged plates. This approach leads to a dramatic speed up of simulations of Coulomb systems confined between charged walls. The dielectric discontinuities can be easily implemented in the present method using periodic images of all the ions,[53] while the electric field produced by the charged surfaces can be replaced by an external potential, as in Eq. (19), but with the dielectric constant of water replaced by the average dielectric constant between the two mediums. Finally, the simulations can be made to run even faster by adopting a Particle-Particle Particle-Mesh (P^3M) approach. Such improvement would allow us to use the algorithm to study all atom simulations of liquid-liquid/vapour interfaces.[54,55]
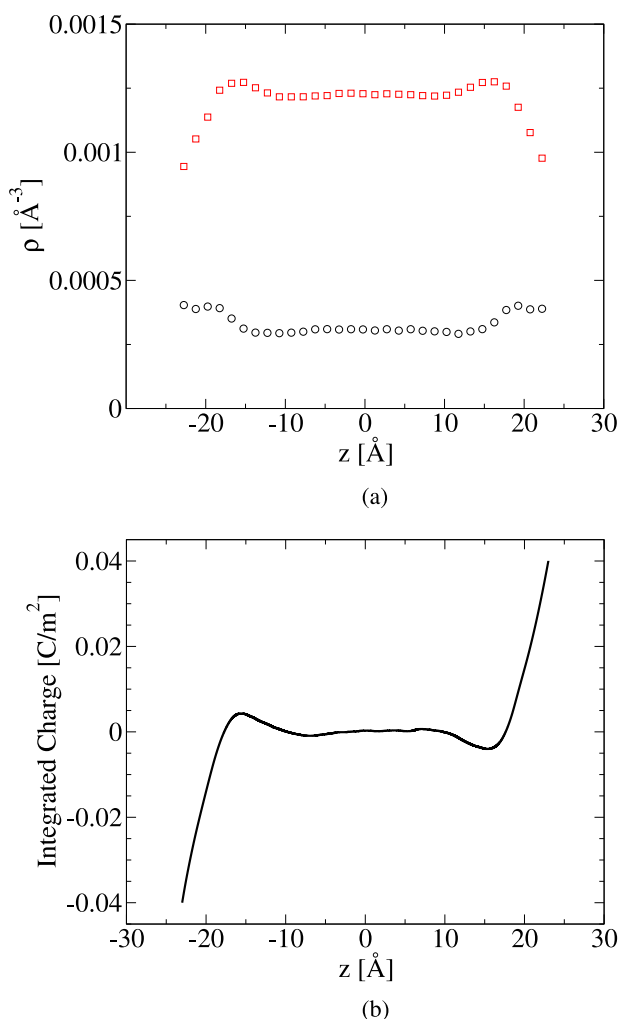

(a)

(b)

FIG. 5. (a) Density profiles of ions between equally charged surfaces confining 4:1 electrolyte—circles represent positive ions, while squares negative ones. (b) The integrated charge.

ACKNOWLEDGMENTS

[1] E. Fitzsimons and J. Sendroy, J. Biol. Chem. **236**, 1595 (1961).
[2] B. K. Korbahti, N. Aktas, and A. Tanyolac, J. Hazard. Mater. **148**, 83 (2007).
[3] H. Uchikawa, S. Hanehara, and D. Sawaki, Cem. Concr. Res. **27**, 37 (1997).
[4] H. Y. Lee and J. B. Goodenough, J. Solid State Chem. **144**, 220 (1999).
[5] M. Winter and R. J. Brodd, Chem. Rev. **104**, 4245 (2004).
[6] Y. Levin, Rep. Prog. Phys. **65**, 1577 (2002).
[7] P. Linse and V. Lobaskin, Phys. Rev. Lett. **83**, 4208 (1999).
[8] A. Diehl, M. N. Tamashiro, M. C. Barbosa, and Y. Levin, Physica A **274**, 433 (1999).
[9] M. M. Hatlo and L. Lue, Europhys. Lett. **89**, 25002 (2010).
[10] L. Samaj and E. Trizac, Phys. Rev. Lett. **106**, 078301 (2011).
[11] A. Martin-Molina, J. G. Ibarra-Armenta, E. Gonzalez-Tovar, R. Hidalgo-Alvarez, and M. Quesada-Perez, Soft Matter **7**, 1441 (2011).
[12] G. N. Patey, J. Chem. Phys. **72**, 5763 (1980).
[13] L. Guldbrand, B. Jonsson, H. Wennerstrom, and P. Linse, J. Chem. Phys. **80**, 2221 (1984).
[14] O. Lenz and C. Holm, Eur. Phys. J. E **26**, 191 (2008).
[15] A. P. dos Santos, A. Diehl, and Y. Levin, J. Chem. Phys. **132**, 104105 (2010).
[16] R. Kjellander and S. Marcelja, J. Phys. Chem. **90**, 1230 (1986).
[17] T. E. Colla, A. P. dos Santos, and Y. Levin, J. Chem. Phys. **136**, 194103 (2012).
[18] R. R. Netz, Eur. Phys. J. E **5**, 557 (2001).
[19] A. G. Moreira and R. R. Netz, Eur. Phys. J. E **8**, 33 (2002).
[20] D. Henderson, S. Lamperski, Z. H. Jin, and J. Z. Wu, J. Phys. Chem. B **115**, 12911 (2011).
[21] M. P. Allen and D. J. Tildesley, *Computer Simulations of Liquids* (Oxford University Press, New York, 1987).
[22] P. Ewald, Ann. Phys. **369**, 253 (1921).
[23] T. Darden, D. York, and L. Pedersen, J. Chem. Phys. **98**, 10089 (1993).
[24] U. Essmann, L. Perera, M. L. Berkowitz, T. Darden, H. Lee, and L. G. Pedersen, J. Chem. Phys. **103**, 8577 (1995).
[25] J. Lekner, Physica A **176**, 485 (1991).
[26] A. H. Widmann and D. B. Adolf, Comput. Phys. Commun. **107**, 167 (1997).
[27] U. Raviv, P. Laurat, and J. Klein, Nature **413**, 51 (2001).
[28] J. Maier, Nat. Mater. **4**, 805 (2005).
[29] Y. F. Jing, V. Jadhao, J. W. Zwanikken, and M. O. de la Cruz, J. Chem. Phys. **143**, 194508 (2015).
[30] C. T. A. Wong and M. Muthukumar, J. Chem. Phys. **126**, 164903 (2007).
[31] P. E. Cazade, R. Hartkamp, and B. Coasne, J. Phys. Chem. C **118**, 5061 (2014).
[32] S. Buyukdagli, J. Phys.: Condens. Matter **27**, 455101 (2015).
[33] K. Hu and A. J. Bard, Langmuir **13**, 5114 (1997).
[34] E. Hackett, E. Manias, and E. P. Giannelis, Chem. Mater. **12**, 2161 (2000).
[35] A. Naji and R. Podgornik, Phys. Rev. E **72**, 041402 (2005).
[36] G. Silbert, D. Ben-Yaakov, Y. Dror, S. Perkin, N. Kampf, and J. Klein, Phys. Rev. Lett. **109**, 168305 (2012).
[37] A. Bakhshandeh, A. P. dos Santos, A. Diehl, and Y. Levin, J. Chem. Phys. **142**, 194707 (2015).
[38] M. Mazars, Mol. Phys. **103**, 1241 (2005).
[39] R. Sperb, Mol. Simul. **13**, 189 (1994).
[40] J. Hautman and M. L. Klein, Mol. Phys. **75**, 379 (1992).
[41] E. Spohr, J. Chem. Phys. **107**, 6342 (1997).
[42] I. C. Yeh and M. L. Berkowitz, J. Chem. Phys. **111**, 3155 (1999).
[43] M. Kawata and M. Mikami, Chem. Phys. Lett. **340**, 157 (2001).
[44] A. Arnold, J. de Joannis, and C. Holm, J. Chem. Phys. **117**, 2496 (2002).
[45] A. Arnold and C. Holm, Chem. Phys. Lett. **354**, 324 (2002).
[46] E. R. Smith, Proc. R. Soc. London, Ser. A **375**, 475 (1981).
[47] D. M. Heyes, J. Chem. Phys. **74**, 1924 (1981).
[48] D. Frenkel and B. Smit, *Understanding Molecular Simulation* (Academic, San Diego, 2002).
[49] T. Laino and J. Hutter, J. Chem. Phys. **129**, 074102 (2008).
[50] J. Stenhammar, M. Trulsson, and P. Linse, J. Chem. Phys. **134**, 224104 (2011).
[51] T. M. Nymand and P. Linse, J. Chem. Phys. **112**, 6152 (2000).
[52] W. B. Russel, D. A. Saville, and W. R. Schowalter, *Colloidal Dispersions* (Cambridge University Press, New York, 1989).
[53] A. P. dos Santos and Y. Levin, J. Chem. Phys. **142**, 194104 (2015).
[54] I. F. W. Kuo, C. J. Mundy, B. L. Eggimann, M. J. McGrath, J. I. Siepmann, B. Chen, J. Vieceli, and D. J. Tobias, J. Phys. Chem. B **110**, 3738 (2006).
[55] B. L. Eggimann and J. I. Siepmann, J. Phys. Chem. C **112**, 210 (2008).